Nano Research

Open Access

Communication

A cellulose-based lithium-ion battery separator with regulated ionic transport and high thermal stability for extreme environments

Kun-Peng Yang[1,§], Song Xie[1,§], Zi-Meng Han[1,§], Hao-Cheng Liu[1], Chong-Han Yin[1], Wen-Bin Sun[1], Zhang-Chi Ling[1], Huai-Bin Yang[1], De-Han Li[1], Qing-Fang Guan[1] ✉, and Shu-Hong Yu[1,2] ✉

[1] *Department of Chemistry, New Cornerstone Science Laboratory, Institute of Biomimetic Materials & Chemistry, Anhui Engineering Laboratory of Biomimetic Materials, Division of Nanomaterials & Chemistry, Hefei National Research Center for Physical Sciences at the Microscale, University of Science and Technology of China, Hefei 230026, China*

[2] *Institute of Innovative Materials, Department of Materials Science and Engineering, Department of Chemistry, Southern University of Science and Technology, Shenzhen 518055, China*

§ *Kun-Peng Yang, Song Xie, and Zi-Meng Han contributed equally to this work.*

Cite this article: *Nano Research*, **2025**, *18*, 94906994. https://doi.org/10.26599/NR.2025.94906994

ABSTRACT: Separators play a critical role in lithium-ion batteries. However, the restrictions of thermal stability and inferior electrical performance in commercial polyolefin separators significantly limit their applications under harsh conditions. Here, we report a cellulose-assisted self-assembly strategy to construct a cellulose-based separator massively and continuously. With an ultrahigh ionic conductivity in electrolytes of 3.7 mS·cm^{-1} and the ability to regulate ion transport, the obtained separator is a promising alternative for high-performance lithium-ion batteries. In addition, integrated with high thermal stability, the cellulose-based separator endows batteries with high safety at high temperatures, greatly expanding the application scenarios of energy storage devices in extreme environments.

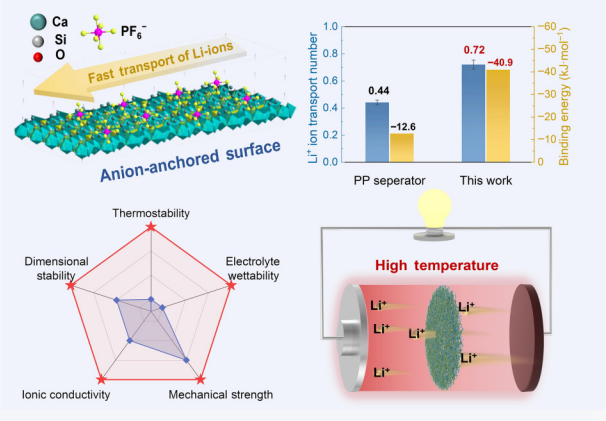

KEYWORDS: lithium-ion batteries, bio-inspired materials, battery separators, cellulose nanofiber, ultrahigh ionic conductivity, high safety

1 Introduction

Nowadays, energy storage equipment is a key technology enabler that plays a vital role in various electronic devices in most application fields, including new energy vehicles, clean energy conversion, and even space exploration [1–5]. Lithium-ion batteries (LIBs) are one of the most widely used energy storage equipment available because of their high energy density and mature production technology [6–8]. However, under many harsh conditions like large-scale energy storage systems, polar regions, space or alien planet exploration, the existing LIBs are hard to meet the needs of these usage scenarios, while they face a series of problems such as decreased performance, prone to failure, and insufficient safety [9–11]. Therefore, there is an urgent need to develop high-performance LIBs that can be highly stable and work efficiently under extreme conditions.

At present, LIBs are generally composed of electrolytes, positive and negative electrodes, and a separator between the electrodes [6]. Among them, the separator plays the role of isolating the positive and negative electrodes to prevent their physical contact that will cause internal short circuits. Meanwhile, it also needs to provide channels for conducting lithium ions in electrolytes to maintain the electrochemical reaction, which is of great importance to the overall safety and efficiency of batteries [12]. The most widely used commercial battery separators are generally polyolefin membranes, such as polypropylene (PP) and polyethylene (PE), due to their high porosity and high electrochemical stability. However, their poor infiltration of electrolytes and lack of ion selective permeation result in poor rate and cycle performance [13]. In the meantime, unsatisfactory thermal stability significantly decreases the safety of

Received: July 14, 2024; **Revised:** August 19, 2024
Accepted: August 19, 2024

✉Address correspondence to Qing-Fang Guan, guanqf@ustc.edu.cn; Shu-Hong Yu, shyu@ustc.edu.cn

LIBs [14, 15]. Thus, many efforts have been made to improve the performance of separators through surface modifications or inorganic nanomaterials coating based on polyolefin separators or replacing polyolefin with other thermally stable materials [16–23]. However, these polyolefin-based materials still face the problem of poor thermal stability, which will make them brittle at low temperatures, shrink and melt at high temperatures, leading to short circuits or even thermal runaway [24, 25]. In addition, ceramic-based separators, nonwoven separators, and paper-based separators are further fabricated with better thermal stability, but the lack of mechanical properties restricts their large-scale applications [19, 26–28]. Therefore, developing battery separators that combine high performance with resistance to extreme environments is hugely crucial to expanding the application scenarios of LIBs.

Herein, we report a homogeneous anion-anchored porous film through a cellulose nanofiber (CNF)-assisted self-assembly strategy. With high porosity, good electrolyte affinity, ultrahigh ionic conductivity, and high thermal stability, the obtained CNF-Xonotlite nanowire (CNF-XNW) film is an ideal material for high-performance high-temperature battery separators. Through binding anions of electrolyte on the surface of the nanochannels in the film, lithium ions released selectively can transport at high speed through abundant interconnected pores inside the film, resulting in high ionic conductive for lithium ions and thus superior cycle and rate performance to the commercial PP separator. In addition, this structure design strategy inherits and enhances the high thermal stability of CNF and XNW, showing no visible change either at high or cold temperatures. It is highly expected to enable LIBs to work safely and efficiently in extreme conditions such as polar exploration and outer space exploration.

2 Results and discussion

A robust CNF-XNW film is fabricated through a scalable CNF-assisted self-assembly strategy. As shown in Fig. 1(a), CNF is extracted by mechanical treatment of bacterial cellulose produced through the biosynthesis of *Acetobacter Xylinum* (Fig. S1 in the Electronic Supplementary Material (ESM)). The CNF obtained possesses superb thermal dimensional stability, high strength, and high hydrophilicity, which is an ideal building block for constructing high-performance films [29–37]. Through forming abundant hydrogen bonds with XNW, CNF can wrap around XNW, thus assisting XNW to be exfoliated from Xonotlite nanowire bundles to form monodisperse nanowires. Subsequently, on account of the abundant hydrogen bonding and van der Waals forces formed between CNF and XNW, a robust film with numerous uniform nanopores is self-assembled with the removal of water (Fig. 1(b), Figs. S2 and S3 in the ESM). This assembly strategy endows the film with substantial pores with good electrolyte wettability, generating a large number of nanochannels that Li-ions can transport through. Furthermore, the surface of the channel has a high affinity for the PF_6^- anions in the electrolyte, promoting the transport of liberated lithium ions (Fig. 1(e)). Combined with other comprehensive performances, including superior thermostability, high dimensional stability, and good mechanical strength to the commercial polyolefin separators (Fig. 1(d)), CNF-XNW is an ideal film material for LIB separators, which can work efficiently and safely under many harsh conditions (Fig. 1(c)). As shown in Fig. 1(f), a soft pack battery equipped with the CNF-XNW separator can power an LED light even in a 150 °C oil bath, while commercial polyolefin separators cannot resist such high temperatures, showing great potential for practical applications in extreme conditions.

Benefiting from high thermal stability, cellulose-based materials are often used to prepare battery separator [19, 28]. However, cellulose-based film usually suffers from poor mechanical strength or unsatisfactory flexibility, making it difficult to achieve high safety for practical production and application. Therefore, it is also highly important to achieve great mechanical properties while ensuring high battery performance. The robust CNF-assisted exfoliation and self-assembly strategy endows the film with superior mechanical and thermal properties. Microscopically, xonotlite nanowire

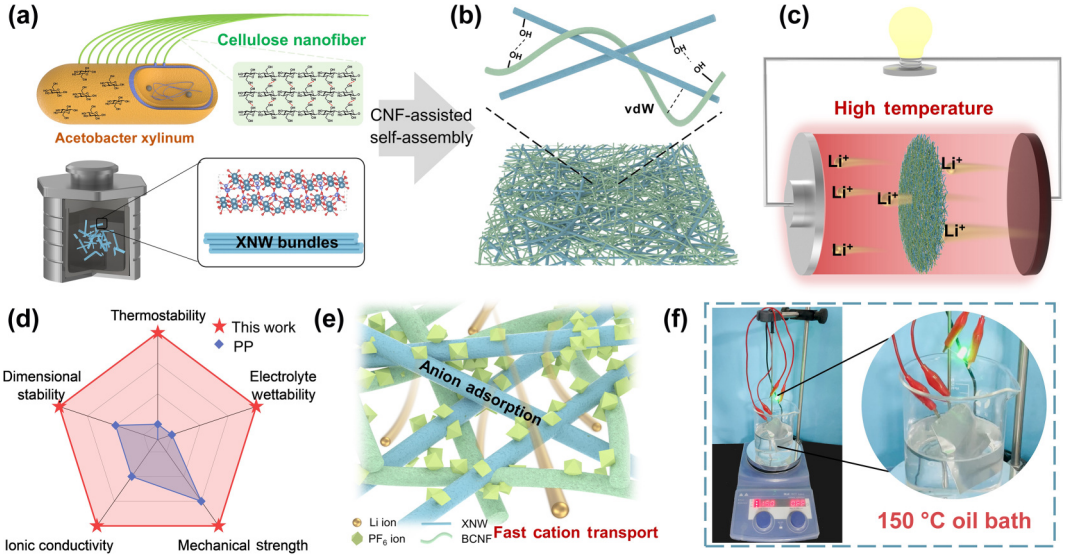

Figure 1 Fabrication and properties of the CNF-XNW separator. (a) CNF is obtained based on biosynthesis, and xonotlite nanowire bundles are fabricated through a hydrothermal process. (b) Xonotlite nanowire bundles are exfoliated into nanowires with the assistance of CNF, self-assembling into a porous double-network film. (c) Illustration of the application as a Li-ion battery separator at high temperature. (d) Comparison with the commonly used PP separator. (e) Schematic diagram of the fast transport of lithium ions through the CNF-XNW separator. (f) A soft pack battery with the CNF-XNW separator discharging at 150 °C.

bundles obtained from the hydrothermal process consist of several aligned nanowires bonded together with low aspect ratios, which are not suitable building blocks for constructing high-performance thin films (Fig. 2(a)). However, under mechanical shearing force, CNF with a high aspect ratio and high density of hydroxyl can wind on the surface of XNW, forming strong hydrogen bonds. Hence, the entanglement of CNF greatly reduces the interactions inside the XNW bundles, assisting in exfoliating XNW bundles into monodisperse nanowires (Fig. 2(b)).

Ulteriorly, Figs. 3(a) and 3(b) suggest that the obtained XNW was well exfoliated after treatment, which is beneficial for enhancing the internal interactions with CNF. Afterwards, intertwined CNF and XNW form a robust high-performance film with a porous network with the removal of water. Benefiting from the interpenetrated nanofiber network and high density of hydrogen bonds as well as van der Waals forces between these nanofibers, the network of the film can absorb a large amount of energy through broken and drawn out of these nanofibers (Figs. 2(c) and 3(c)). Hence, the inherent high strength properties of CNF are amplified into macroscopic film materials, endowing the film with high strength, high flexibility and high modulus. Compared with the low strength in the transverse direction of anisotropic commercial PP separators, CNF-XNW shows an isotropic high strength of 53 MPa and a high modulus of 2.03 GPa (Figs. 2(d) and 2(e)), ensuring the integrity of the separator during the winding of film production and battery assembly. Furthermore, during the scalable production of LIBs, the uneven electrode surface or the entry of tiny dust may cause the puncture of the separator, resulting in a severe internal short circuit [27]. CNF-XNW with much higher hardness than PP separators possesses better resistance to microscopic puncture, significantly reducing the safety hazard of batteries.

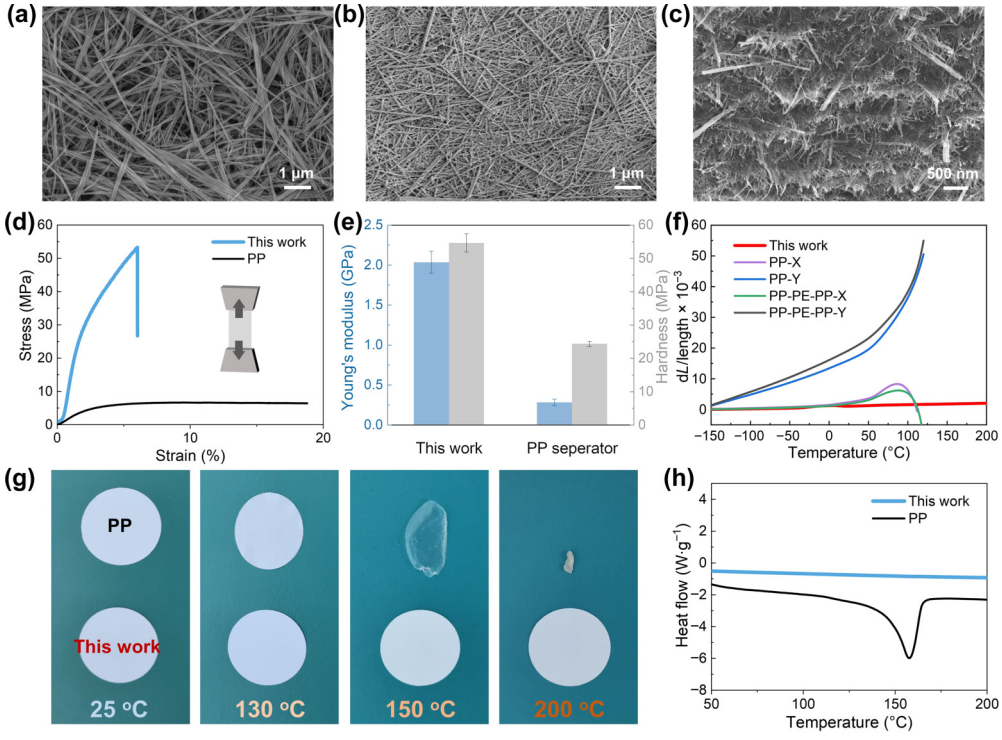

Figure 2 Superb mechanical and thermal properties of the CNF-XNW separator. (a) Scanning electron microscopy (SEM) image of XNW bundles. (b) SEM image of the CNF-XNW separator. (c) SEM image of the fracture of the CNF-XNW separator, showing breakage and extraction of fibers. (d) The flexural stress–strain curves of the CNF-XNW separator compared with the transverse direction of a commonly used PP separator. (e) High modulus and hardness of CNF-XNW compared with the PP separator. (f) Comparison of thermal expansion with the PP and PP-PE-PP separators from −150 to 200 °C. X presents the machine direction and Y presents the transverse direction. (g) Hot plate test of the CNF-XNW separator and the PP separator. (h) DSC curves of the CNF-XNW separator and the PP separator.

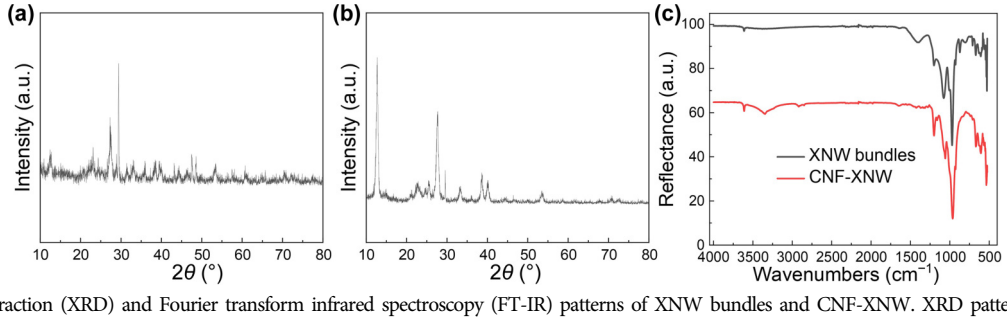

Figure 3 X-ray diffraction (XRD) and Fourier transform infrared spectroscopy (FT-IR) patterns of XNW bundles and CNF-XNW. XRD patterns of the (a) XNW bundles and (b) CNF-XNW, illustrating the XNW bundles are exfoliated into nanowires. (c) FT-IR patterns of XNW bundles and CNF-XNW, showing high density of hydrogen bonds in the CNF-XNW film.

Additionally, thermostability and dimensional stability of the separator are particularly critical to maintaining safety during cycling and expanding the working range of batteries [26]. Although polyolefin separators can achieve thermal shutdown through closing pores along the battery temperature rising, the shutdown temperature is very close to the deformation temperature [38]. Thus, when the internal temperature rises due to thermal inertia, the widely used polyolefin-based separators may undergo severe shrinkage and deformation at high temperatures, resulting in direct contact between the positive and negative electrodes to cause severe internal short circuits and thermal runaway [39]. In particular, polyolefin separators with stretched pores possess a large thermal expansion coefficient, deforming significantly at high temperatures. In contrast, the advantages of the low thermal expansion coefficient of CNF and XNW are inherited and enhanced in CNF-XNW separators. Thus, CNF-XNW has an average thermal expansion coefficient of lower than 7×10^{-6} K^{-1} from −150 to 200 °C, while commercial PP and PP-PE-PP separators possess a much higher average thermal expansion coefficients, especially along the transverse direction (Fig. 2(f)). The superiority in dimensional stability of CNF-XNW compared to polyolefin separators progressively becomes more pronounced as the temperature increases, illustrating the great application potential in extreme temperature environments. As shown in Fig. 2(g), as the temperature increases from 25 to 200 °C, the PP separator gradually shrinks and deforms unevenly, eventually melts, while CNF-XNW shows no significant change all along, demonstrating its remarkable thermal dimensional stability. The differential scanning calorimetry (DSC) curves further reveal that no melt or decomposition of CNF-XNW occurs in this temperature range, yet the PP separator starts to melt and absorbs energy significantly from 150 °C (Fig. 2(h)). Furthermore, the CNF-XNW separator maintains remarkable flexibility even in liquid nitrogen of −196 °C or under the burning of an alcohol flame of ~ 500 °C (Movie S1 in the ESM). Astonishingly, attributed to the construction of the organic–inorganic nanofiber network, even under the burning of butane flame with a high temperature reaching ~ 1300 °C, unlike pure organic films will burn completely, the CNF-XNW separator can keep its original shape (Fig. S4 in the ESM), which means even if the battery is burned due to external accident, CNF-XNW separators can also play the role in separating the positive and negative electrodes to minimize the risk of further short circuit and heat release.

Besides preventing the positive and negative electrodes from directly contacting, one of the most important roles of separators is to conduct lithium ions and maintain the electrochemical reaction inside cells, which greatly influence the cycle and rate performance [40]. Benefiting from the CNF-assisted self-assembly strategy, a porous network of the CNF-XNW separator is constructed through the entanglement and interpenetration of CNF with XNW, producing abundant nanopores mainly sized from 6 to 20 nm, which act as nano-sized channels for Li-ions to transport through (Figs. 4(a) and 4(b)). Contact angle measurements and electrolyte uptake tests were further performed to illustrate that the porous structure composed of CNF-XNW has improved infiltration and adsorption to the electrolyte, which is beneficial for both conducting ions and decreasing the cost through accelerating the wetting process. On the one hand, the CNF-XNW separator has

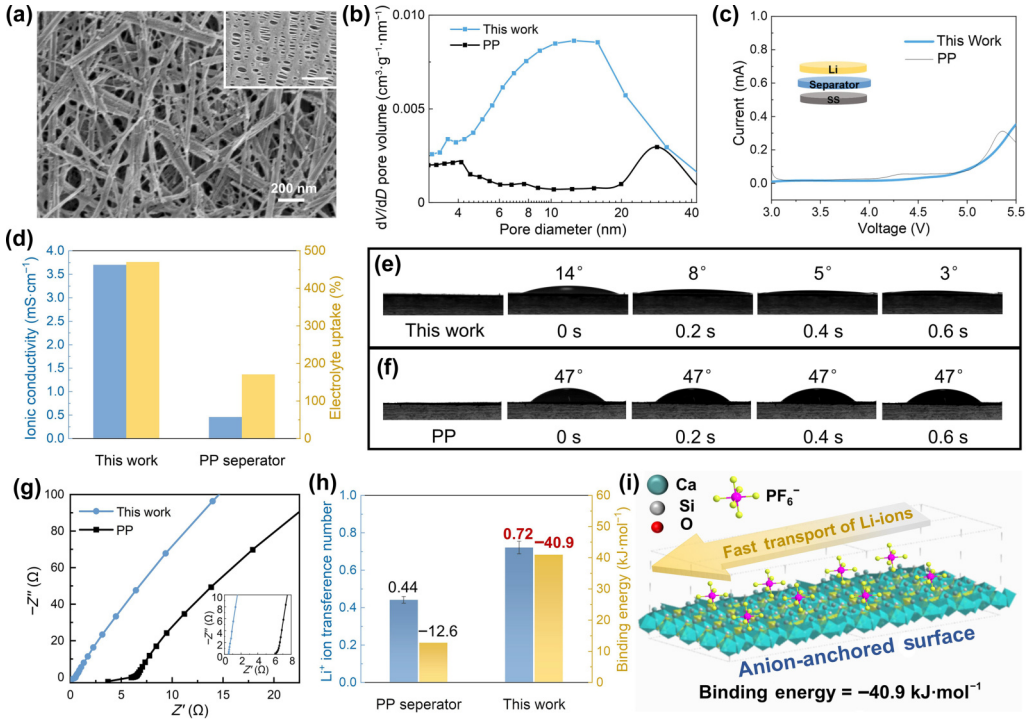

Figure 4 Li-ion conductive properties of the CNF-XNW separator. (a) The pore structure of the CNF-XNW separator compared with the PP separator. The inset scale bar is 500 nm. (b) Pore size distribution of the CNF-XNW and PP separators. (c) Electrochemical impedance spectroscopy (EIS) of symmetric stainless steel (SS)/separator/SS cells at 25 °C for the calculation of ionic conductivity. (d) Comparison of ionic conductivity and electrolyte uptake between the CNF-XNW and PP separators. Surface electrolyte contact angles of (e) CNF-XNW and (f) PP. (g) Linear sweep voltammetry (LSV) curves of the CNF-XNW and PP separator, showing high electrochemical stability of the CNF-XNW separator. (h) Comparison of Li-ion transport number and calculated binding energy between PF_6^- anions and the separators. (i) Schematic of fast transport of Li-ions on the anion-anchored surface inside the CNF-XNW separator.

outstanding wettability to the electrolyte, showing an extremely small contact angle of the electrolyte (Fig. 4(e)). Thus, the electrolyte droplets are fully diffused on the surface of the CNF-XNW separator. On the other hand, the electrolyte is quickly absorbed into the interconnected porous network, reaching a high electrolyte uptake of 450% (Fig. 4(d)), which mainly indicates better affinity for electrolyte compared to PP, thus, leading to enhanced ion transport properties [41]. Furthermore, the electrochemical stability of separators is of significant importance for the operating voltage range of the battery. Observed from the linear sweep voltammetry of SS/separator/Li cells (Fig. 4(c)), CNF-XNW shows a stable current under 4.5 V while the PP separator becomes unstable at approximately 4.2 V, indicating higher electrochemical stability compared to the PP separator.

To evaluate the ionic conductive ability of CNF-XNW separators with electrolytes quantitatively, EIS of symmetric cells composed of SS/separator/SS was acquired and analyzed. Remarkably, the ionic conductivity of CNF-XNW with electrolytes reaches 3.7 mS·cm^{-1}, which is more than eight times that of the PP separator (Fig. 4(g)), demonstrating an ultrahigh ionic conductive ability in electrolyte among other recently reported separators (Table S1 in the ESM). Generally, the key factors of separators affecting the ionic conductivity in LIBs mainly contain the affinity to electrolytes and the pore structure inside the separator [42]. In the nature, plant cell walls with abundant hydrophilic cellulose, play an important role in the transport of water and the dissolved mineral ions [43, 44]. In particular, the interconnected cell wall structure and the capillary action of the hydrophilic channels enhance the transport of dissolved substances and water in xylem conduits [45–47]. Similarly, inside the CNF-XNW separator, CNF with good electrolyte wettability enables the electrolyte to fully infiltrate the large number of interconnected nanopores constructed by the assembly of CNF and XNW, building a mass of channels that can effectively transport ions. Consequently, CNF-XNW separators have exceptional ionic conductivity, which is superior to any polyolefin-based separators. As a comparison, the contact angle of the electrolyte with the PP separator is 47° (Fig. 4(f)), which is much higher than that of CNF-XNW. Thus, the poor wettability to the electrolyte and the discrete stretched of the PP separator cause poor electrolyte infiltration in the pores, resulting in a large number of ineffective pores [48, 49]. Therefore, the ineffective pores greatly limit the formation of ion-conducting pathways, resulting in lower ionic conductivity.

Interestingly, the CNF-XNW separator not only has excellent wettability to the solvent components of the electrolyte, but also has a good anchorage to the fluorine-containing anions in the electrolyte. Density functional theory (DFT) calculation is performed to evaluate the binding of PF_6^- anions with CNF-XNW and PP separators respectively. The binding energy of PF_6^- ions with the exposed facets of XNW reaches −40.9 kJ·mol^{-1}, which is approximately 3.2 times that of PP, indicating strong interactions among PF_6^- anions and the CNF-XNW separator (Fig. 4(h)). Thus, PF_6^- anions prefer to anchor onto the network of the CNF-XNW separator, liberating more Li-ions in the electrolyte [50, 51]. Consequently, during the drive of the potential difference, lithium ions can rapidly migrate on the anion-anchored surface of the abundant channels inside the CNF-XNW separator (Fig. 4(i)).

To further confirm the ion transport regulation ability of CNF-XNW, the Bruce-Vincent method is applied to quantify the Li-ion transport number, which is a useful parameter for evaluating the Li-ion transport properties [52, 53]. Although the Bruce-Vincent method is often used to approximate ion transference number in polymer electrolytes without ion association, it will overestimate the lithium ion transference number when applied to high concentration liquid electrolytes [54]. Therefore, the measured data is called Li-ion transport number to be more accurate and can reflect the impact on ion transport [55]. Attributed to the high binding energy between the CNF-XNW separator and PF_6^- anions, the Li-ion transport number of CNF-XNW is approximately 1.6 times that of PP separators with weaker binding energy to PF_6^- anions (Fig. 4(h), Fig. S5 and Table S2 in the ESM). Typically, a low Li-ion transport number causes a large number of anions to accumulate on the electrode surface, resulting in an accumulation of concentration gradients [56, 57]. As a consequence, it severely limits the rate performance during the charge and discharge of LIBs. Therefore, the boosting of Li-ion migration of CNF-XNW by regulating ion transport greatly enhances the charge–discharge performance of lithium-ion batteries, which can significantly improve the fast-charging performance and energy density of LIBs.

Integrated with high ionic conductivity, high Li-ion transport number, and high thermal stability, CNF-XNW is a promising separator for enhancing LIBs in both performance and safety. Thus, a series of batteries equipped with CNF-XNW separators were assembled to demonstrate the practical application potential. $LiFePO_4$/separator/Li cells were assembled to evaluate the electrochemical performance. Benefiting from the high ionic conductivity, which reduces the energy loss during Li-ions transport, the battery equipped with the CNF-XNW separator not only has a higher initial capacity than that of the PP separator but also has a superior capacity retention rate of ~ 90% after 300 cycles, while the battery equipped with the PP separator only maintains less than 20% compared to the initial capacity (Fig. 5(a)).

Furthermore, due to the appropriate regulation of ions in electrolytes, the battery with CNF-XNW as a separator shows remarkable rate performance. At the cycle rates of 0.1, 0.2, 0.3, 0.5, 1, 2, 3, and 5 C of $LiFePO_4$/separator/Li cells, CNF-XNW cells have higher capacity than PP cells constantly (Fig. 5(b)). Especially at the rate of 5 C, CNF-XNW cells maintain a high specific capacity of about 80 mAh·g^{-1}, while PP cells only have a specific capacity of lower than 50 mAh·g^{-1} contrastively.

In addition, full-cell tests were further conducted to demonstrate the advantages of CNF-XNW for a broader range of practical applications. Under the same test conditions, CNF-XNW separators still provide the batteries with significant capacity retention during long-term cycling at 1 C and outstanding specific capacity in rate tests compared to PP separator (Figs. 5(d) and 5(e)). At a high charge–discharge rate of 5 C, the battery with the CNF-XNW separator maintains an extraordinary specific capacity of around 75 mAh·g^{-1}, which is about seven times that of the battery with a PP separator. Over and above, after cycling for 100 and 500 cycles, the CNF-XNW separator endows the battery with a high specific capacity of about 111 and 100 mAh·g^{-1}. In contrast, the battery with a PP separator only possesses a low specific capacity of approximately 80 and even 30 mAh·g^{-1} respectively (Fig. 5(f) and Fig. S6 in the ESM). The improvement in cycling may be attributed to that the higher electrolyte affinity and ionic conductivity of the

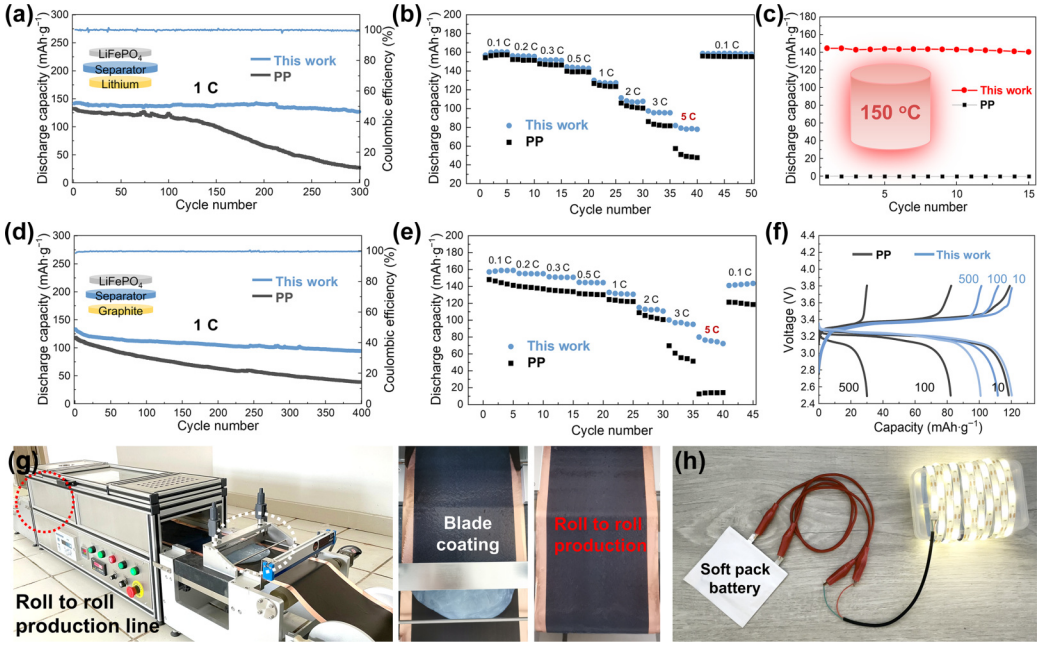

Figure 5 CNF-XNW separators improving the electrochemical performance of Li-ion batteries. (a) $LiFePO_4$/separator/Li cells galvanostatic cycling at 1 C (initial five cycles at 0.1 C). (b) Rate performance at 0.1, 0.2, 0.3, 0.5, 1, 2, 3, and 5 C of $LiFePO_4$/separator/Li cells. (c) $LiFePO_4$/separator/Li cells galvanostatic cycling at 1 C at 150 °C. (d) $LiFePO_4$/separator/graphite cells galvanostatic cycling at 1 C (initial five cycles at 0.1 C). (e) Rate performance of $LiFePO_4$/separator/graphite cells. (f) The charge–discharge curves of LIBs equipped with CNF-XNW and PP separators at 1 C during the long-term cycle (initial five cycles at 0.1 C). (g) Roll-to-roll equipment for the production of the CNF-XNW separator. (h) Soft pack battery equipped with the CNF-XNW separator powering a roll of the light strip.

CNF-XNW separator result in lower interfacial resistance, reducing additional energy consumption during cycling and improving the battery cycle life [58]. Hence, the CNF-XNW separator is a promising alternative for constructing long-life fast-charging LIBs.

More importantly, in the practical applications of batteries, external high-temperature conditions, unstable voltages, mechanical shocks, system errors, aging of electrolytes, etc. may lead to an increase in the overall temperature of the battery. As the temperature of the battery increases, traditional polyolefin separators come across the problem of shrinkage and melting, which may lead to an internal short circuit. Consequently, a large amount of heat may be generated in a short time, resulting in severe problems such as a thermal runaway. On the contrary, CNF-XNW with high thermal stability and thermal dimensional stability endows batteries with remarkable resistance to high temperatures. As shown in Fig. 5(c), in the high-temperature environment of 150 °C, the battery assembled with the PP separator lost efficacy immediately, due to the separator was damaged at this high temperature and could no longer work (Figs. S7(c) and S7(d) in the ESM). However, owing to the fact that the CNF-XNW separator does not shrink or decompose at high temperatures (Figs. S7(a) and S7(b) in the ESM), preventing the occurrence of direct contact of electrodes, the battery with the CNF-XNW separator still cycled normally with a high capacity, significantly improving the overall safety of LIBs, which shows great application potential in the field of high-temperature batteries.

Through these series of battery tests above, it is strongly proven that the CNF-XNW separator significantly enhances the cycle and rate performance of LIBs, as well as enables the batteries to work at high temperatures. However, how to achieve the large-scale production and wide practical application of high-performance separators has always been a huge challenge. For example, polyimide-based separators with excellent thermal stability and electrolyte affinity, have received a lot of attention [58–60]. But how to realize industrial fabrication and low-cost commercial production remains a urgent problem due to the lack of mechanical strength of polyimide-based separators (Table S1 in the ESM) and the complex production process [60]. In order to verify the large-scale preparation and application potentials of the CNF-XNW separator, a set of continuous blade coating roll-to-roll equipment for the scalable production of CNF-XNW separators is well designed and constructed (Fig. 5(g)). Firstly, a thin layer of CNF-XNW slurry is blade coated on the commercial negative electrode substrate. Afterwards, a drying tunnel of 80 °C is applied to remove water content for the self-assembly of CNF-XNW separators on the substrate. With additional rewinding and rolling processes, the composite film of the negative electrode and the CNF-XNW separator is obtained continuously. Additionally, soft pack batteries equipped with CNF-XNW separators were further assembled for indicating practical large-scale applications. As shown in Fig. 5(h) and Movie S2 in the ESM, a roll of an LED light strip is powered by a CNF-XNW soft pack battery, demonstrating the great potential for applications in the fields of large-scale high-density lithium batteries and energy storage equipment.

3 Conclusion

In summary, a cellulose-based high-performance battery separator with ultrahigh and selective ionic conductivity, superb ion regulation ability, and superior thermal stability is fabricated through a CNF-assisted self-assembly strategy. Such a CNF-XNW separator possesses high-density and uniform interconnected nano-scale pores, with high affinity for electrolyte and strong binding to anions, endows batteries with outstanding rate and cycle performance. Furthermore, the CNF-XNW separator is highly stable in structure and performance under the harsh environment of high temperature, ensuring both high electrochemical performance and high safety of batteries, making great

contributions to expanding the application scenarios of energy storage devices. With advanced electrolytes and improved electrodes in the future, this new kind of CNF-XNW separators is expected to have significant applications in extreme environments such as outer space exploration and alien planet settlement.

Electronic Supplementary Material: Supplementary material (Methods; SEM image of the CNF, photograph of the CNF-XNW separator, SEM image of the cross-section of the CNF-XNW separator, fire-resistant property of the CNF-XNW separator, Li-ion transport number measurements of the CNF-XNW separator, the charge–discharge curves of LIBs equipped with CNF-XNW separators during 1 C cycling, SEM images of separators before and after high-temperature battery tests; Comparison of electrochemical performances and mechanical strength of the CNF-XNW separator with recently reported separators for LiBs, the parameters for calculating Li-ion transport number; CNF-XNW separators bending under liquid nitrogen and alcohol flame, and a roll of an LED light strip powered by a CNF-XNW soft pack battery) is available in the online version of this article at https://doi.org/10.26599/NR.2025.94906994.

Data availability

All data needed to support the conclusions in the paper are presented in the manuscript and the Electronic Supplementary Material. Additional data related to this paper may be requested from the corresponding author upon request.

Acknowledgements

This work was supported by the Strategic Priority Research Program of the Chinese Academy of Sciences (No. XDB0450402), the National Key Research and Development Program of China (Nos. 2018YFE0202201 and 2021YFA0715700), the National Natural Science Foundation of China (Nos. 22293044, U1932213, 51732011, 22105194, and 92163130), the Major Basic Research Project of Anhui Province (No. 2023z04020009), and the New Cornerstone Investigator Program. This work was partially carried out at the USTC Center for Micro and Nanoscale Research and Fabrication. We thank Ming Li, Sheng-Quan Fu, and Hong-Min Zhou from the Instruments Center for Physical Science, University of Science and Technology of China for help with the SEM characterization. The Super Computing Center of USTC is gratefully acknowledged.

Declaration of competing interest

All the contributing authors report no conflict of interests in this work. Author Shu-Hong Yu is the editorial board member of this journal, but he is not involved in the peer-review or decision of this article.

Author contribution statement

Q.-F. G. and S.-H. Y. conceived the idea and designed the experiments. S.-H. Y. and Q.-F. G. supervised the project. K.-P. Y., S. X., Z.-M. H., H.-C. L., C.-H. Y., W.-B. S., H.-B. Y., Z.-C. L., and D.-H. L. carried out the fabrication experiment and analysis. K.-P. Y. and C.-H. Y. contributed to the 3D illustration. K.-P. Y., S. X., Z.-M. H., Q.-F. G., and S.-H. Y. wrote the paper, and all authors discussed the results and commented on the manuscript.

Use of AI statement

None.

References

[1] Dunn, B.; Kamath, H.; Tarascon, J. M. Electrical energy storage for the grid: A battery of choices. *Science* **2011**, *334*, 928–935.
[2] Arbabzadeh, M.; Sioshansi, R.; Johnson, J. X.; Keoleian, G. A. The role of energy storage in deep decarbonization of electricity production. *Nat. Commun.* **2019**, *10*, 3413.
[3] Pomerantseva, E.; Bonaccorso, F.; Feng, X. L.; Cui, Y.; Gogotsi, Y. Energy storage: The future enabled by nanomaterials. *Science* **2019**, *366*, eaan8285.
[4] Zheng, J. X.; Archer, L. A. Controlling electrochemical growth of metallic zinc electrodes: Toward affordable rechargeable energy storage systems. *Sci. Adv.* **2021**, *7*, eabe0219.
[5] Jones, J. P.; Smart, M. C.; Krause, F. C.; West, W. C.; Brandon, E. J. Batteries for robotic spacecraft. *Joule* **2022**, *6*, 923–928.
[6] Goodenough, J. B.; Park, K. S. The Li-ion rechargeable battery: A perspective. *J. Am. Chem. Soc.* **2013**, *135*, 1167–1176.
[7] Yoshino, A. The birth of the lithium-ion battery. *Angew. Chem., Int. Ed.* **2012**, *51*, 5798–5800.
[8] Yang, C. P.; Wu, Q. S.; Xie, W. Q.; Zhang, X.; Brozena, A.; Zheng, J.; Garaga, M. N.; Ko, B. H.; Mao, Y. M.; He, S. M. et al. Copper-coordinated cellulose ion conductors for solid-state batteries. *Nature* **2021**, *598*, 590–596.
[9] Manthiram, A. Materials challenges and opportunities of lithium ion batteries. *J. Phys. Chem. Lett.* **2011**, *2*, 176–184.
[10] Kuang, Y. D.; Chen, C. J.; Pastel, G.; Li, Y. J.; Song, J. W.; Mi, R. Y.; Kong, W. Q.; Liu, B. Y.; Jiang, Y. Q.; Yang, K. et al. Conductive cellulose nanofiber enabled thick electrode for compact and flexible energy storage devices. *Adv. Energy Mater.* **2018**, *8*, 1802398.
[11] Nitta, N.; Wu, F. X.; Lee, J. T.; Yushin, G. Li-ion battery materials: Present and future. *Mater. Today* **2015**, *18*, 252–264.
[12] Zhang, S. S. A review on the separators of liquid electrolyte Li-ion batteries. *J. Power Sources* **2007**, *164*, 351–364.
[13] Francis, C. F. J.; Kyratzis, I. L.; Best, A. S. Lithium-ion battery separators for ionic-liquid electrolytes: A review. *Adv. Mater.* **2020**, *32*, 1904205.
[14] Wang, L.; Ma, Z. L.; Zhang, Y. L.; Chen, L. X.; Cao, D. P.; Gu, J. W. Polymer-based EMI shielding composites with 3D conductive networks: A mini-review. *SusMat* **2021**, *1*, 413–431.
[15] Eng, A. Y. S.; Soni, C. B.; Lum, Y.; Khoo, E.; Yao, Z. P.; Vineeth, S. K.; Kumar, V.; Lu, J.; Johnson, C. S.; Wolverton, C. et al. Theory-guided experimental design in battery materials research. *Sci. Adv.* **2022**, *8*, eabm2422.
[16] Zheng, H.; Wang, Z. Y.; Shi, L. Y.; Zhao, Y.; Yuan, S. Enhanced thermal stability and lithium ion conductivity of polyethylene separator by coating colloidal SiO_2 nanoparticles with porous shell. *J. Colloid Interface Sci.* **2019**, *554*, 29–38.
[17] Nunes-Pereira, J.; Costa, C. M.; Lanceros-Méndez, S. Polymer composites and blends for battery separators: State of the art, challenges and future trends. *J. Power Sources* **2015**, *281*, 378–398.
[18] Woo, J. J.; Zhang, Z. C.; Dietz Rago, N. L.; Lu, W. Q.; Amine, K. A high performance separator with improved thermal stability for Li-ion batteries. *J. Mater. Chem. A* **2013**, *1*, 8538–8540.
[19] Li, H.; Wu, D. B.; Wu, J.; Dong, L. Y.; Zhu, Y. J.; Hu, X. L. Flexible, high-wettability and fire-resistant separators based on hydroxyapatite nanowires for advanced lithium-ion batteries. *Adv. Mater.* **2017**, *29*, 1703548.
[20] Evans, T.; Lee, J. H.; Bhat, V.; Lee, S. H. Electrospun polyacrylonitrile microfiber separators for ionic liquid electrolytes in Li-ion batteries. *J. Power Sources* **2015**, *292*, 1–6.

[21] Pan, Y. D.; Chou, S. L.; Liu, H. K.; Dou, S. X. Functional membrane separators for next-generation high-energy rechargeable batteries. *Natl. Sci. Rev.* **2017**, *4*, 917–933.
[22] Zhang, T. W.; Chen, J. L.; Tian, T.; Shen, B.; Peng, Y. D.; Song, Y. H.; Jiang, B.; Lu, L. L.; Yao, H. B.; Yu, S. H. Sustainable separators for high-performance lithium ion batteries enabled by chemical modifications. *Adv. Funct. Mater.* **2019**, *29*, 1902023.
[23] Nestler, T.; Schmid, R.; Münchgesang, W.; Bazhenov, V.; Schilm, J.; Leisegang, T.; Meyer, D. C. Separators-technology review: Ceramic based separators for secondary batteries. *AIP Conf. Proc.* **2014**, *1597*, 155–184.
[24] Lee, H.; Yanilmaz, M.; Toprakci, O.; Fu, K.; Zhang, X. W. A review of recent developments in membrane separators for rechargeable lithium-ion batteries. *Energy Environ. Sci.* **2014**, *7*, 3857–3886.
[25] Huang, X. S. Separator technologies for lithium-ion batteries. *J. Solid State Electrochem.* **2011**, *15*, 649–662.
[26] Lagadec, M. F.; Zahn, R.; Wood, V. Characterization and performance evaluation of lithium-ion battery separators. *Nat. Energy* **2019**, *4*, 16–25.
[27] Halalay, I. C.; Lukitsch, M. J.; Balogh, M. P.; Wong, C. A. Nanoindentation testing of separators for lithium-ion batteries. *J. Power Sources* **2013**, *238*, 469–477.
[28] Jia, S. J.; Yang, S. H.; Zhang, M. Q.; Huang, K. L.; Long, J. T.; Xiao, J. Eco-friendly xonotlite nanowires/wood pulp fibers ceramic hybrid separators through a simple papermaking process for lithium ion battery. *J. Membr. Sci.* **2020**, *597*, 117725.
[29] Podsiadlo, P.; Kaushik, A. K.; Arruda, E. M.; Waas, A. M.; Shim, B. S.; Xu, J. D.; Nandivada, H.; Pumplin, B. G.; Lahann, J.; Ramamoorthy, A. et al. Ultrastrong and stiff layered polymer nanocomposites. *Science* **2007**, *318*, 80–83.
[30] Munch, E.; Launey, M. E.; Alsem, D. H.; Saiz, E.; Tomsia, A. P.; Ritchie, R. O. Tough, bio-inspired hybrid materials. *Science* **2008**, *322*, 1516–1520.
[31] Nogi, M.; Yano, H. Transparent nanocomposites based on cellulose produced by bacteria offer potential innovation in the electronics device industry. *Adv. Mater.* **2008**, *20*, 1849–1852.
[32] Fukuzumi, H.; Saito, T.; Iwata, T.; Kumamoto, Y.; Isogai, A. Transparent and high gas barrier films of cellulose nanofibers prepared by TEMPO-mediated oxidation. *Biomacromolecules* **2009**, *10*, 162–165.
[33] Guan, Q. F.; Ling, Z. C.; Han, Z. M.; Yang, H. B.; Yu, S. H. Ultra-strong, ultra-tough, transparent, and sustainable nanocomposite films for plastic substitute. *Matter* **2020**, *3*, 1308–1317.
[34] Nogi, M.; Iwamoto, S.; Nakagaito, A. N.; Yano, H. Optically transparent nanofiber paper. *Adv. Mater.* **2009**, *21*, 1595–1598.
[35] Guan, Q. F.; Yang, H. B.; Han, Z. M.; Zhou, L. C.; Zhu, Y. B.; Ling, Z. C.; Jiang, H. B.; Wang, P. F.; Ma, T.; Wu, H. A. et al. Lightweight, tough, and sustainable cellulose nanofiber-derived bulk structural materials with low thermal expansion coefficient. *Sci. Adv.* **2020**, *6*, eaaz1114.
[36] Meyers, M. A.; McKittrick, J.; Chen, P. Y. Structural biological materials: Critical mechanics-materials connections. *Science* **2013**, *339*, 773–779.
[37] Guan, Q. F.; Yang, K. P.; Han, Z. M.; Yang, H. B.; Ling, Z. C.; Yin, C. H.; Yu, S. H. Sustainable multiscale high-haze transparent cellulose fiber film via a biomimetic approach. *ACS Mater. Lett.* **2022**, *4*, 87–92.
[38] Liu, Z. F.; Jiang, Y. J.; Hu, Q. M.; Guo, S. T.; Yu, L.; Li, Q.; Liu, Q.; Hu, X. L. Safer lithium-ion batteries from the separator aspect: Development and future perspectives. *Energy Environ. Mater.* **2021**, *4*, 336–362.
[39] Liu, Z. F.; Peng, Y. T.; Meng, T.; Yu, L.; Wang, S.; Hu, X. L. Thermal-triggered fire-extinguishing separators by phase change materials for high-safety lithium-ion batteries. *Energy Storage Mater.* **2022**, *47*, 445–452.
[40] Zhang, T. W.; Tian, T.; Shen, B.; Song, Y. H.; Yao, H. B. Recent advances on biopolymer fiber based membranes for lithium-ion battery separators. *Compos. Commun.* **2019**, *14*, 7–14.
[41] Wang, Y.; Guo, M. H.; Fu, H.; Wu, Z. Z.; Zhang, Y. Z.; Chao, G. J.; Chen, S. L.; Zhang, L. S.; Liu, T. X. Thermotolerant separator of cross-linked polyimide fibers with narrowed pore size for lithium-ion batteries. *J. Membr. Sci.* **2022**, *662*, 121004.
[42] Lagadec, M. F.; Zahn, R.; Müller, S.; Wood, V. Topological and network analysis of lithium ion battery components: The importance of pore space connectivity for cell operation. *Energy Environ. Sci.* **2018**, *11*, 3194–3200.
[43] Cosgrove, D. J. Growth of the plant cell wall. *Nat. Rev. Mol. Cell Biol.* **2005**, *6*, 850–861.
[44] Varner, J. E.; Lin, L. S. Plant cell wall architecture. *Cell* **1989**, *56*, 231–239.
[45] Nardini, A.; Lo Gullo, M. A.; Salleo, S. Refilling embolized xylem conduits: Is it a matter of phloem unloading. *Plant Sci.* **2011**, *180*, 604–611.
[46] Steudle, E.; Frensch, J. Water transport in plants: Role of the apoplast. *Plant Soil* **1996**, *187*, 67–79.
[47] Sattelmacher, B. The apoplast and its significance for plant mineral nutrition. *New Phytol.* **2001**, *149*, 167–192.
[48] Xie, Y.; Zou, H. L.; Xiang, H. F.; Xia, R.; Liang, D. D.; Shi, P. C.; Dai, S.; Wang, H. H. Enhancement on the wettability of lithium battery separator toward nonaqueous electrolytes. *J. Membr. Sci.* **2016**, *503*, 25–30.
[49] l'Abee, R.; DaRosa, F.; Armstrong, M. J.; Hantel, M. M.; Mourzagh, D. High temperature stable Li-ion battery separators based on polyetherimides with improved electrolyte compatibility. *J. Power Sources* **2017**, *345*, 202–211.
[50] Wang, J.; Liu, Y. P.; Cai, Q. F.; Dong, A. G.; Yang, D.; Zhao, D. Y. Hierarchically porous silica membrane as separator for high-performance lithium-ion batteries. *Adv. Mater.* **2022**, *34*, 2107957.
[51] Zhang, C.; Shen, L.; Shen, J. Q.; Liu, F.; Chen, G.; Tao, R.; Ma, S. X.; Peng, Y. T.; Lu, Y. F. Anion-sorbent composite separators for high-rate lithium-ion batteries. *Adv. Mater.* **2019**, *31*, 1808338.
[52] Evans, J.; Vincent, C. A.; Bruce, P. G. Electrochemical measurement of transference numbers in polymer electrolytes. *Polymer* **1987**, *28*, 2324–2328.
[53] Galluzzo, M. D.; Maslyn, J. A.; Shah, D. B.; Balsara, N. P. Ohm's law for ion conduction in lithium and beyond-lithium battery electrolytes. *J. Chem. Phys.* **2019**, *151*, 020901.
[54] Hallinan, D. T.; Villaluenga, I.; Balsara, N. P. Polymer and composite electrolytes. *MRS Bull.* **2018**, *43*, 759–767.
[55] Mittal, N.; Ojanguren, A.; Cavasin, N.; Lizundia, E.; Niederberger, M. Transient rechargeable battery with a high lithium transport number cellulosic separator. *Adv. Funct. Mater.* **2021**, *31*, 2101827.
[56] Zahn, R.; Lagadec, M. F.; Hess, M.; Wood, V. Improving ionic conductivity and lithium-ion transference number in lithium-ion battery separators. *ACS Appl. Mater. Interfaces* **2016**, *8*, 32637–32642.
[57] Diederichsen, K. M.; McShane, E. J.; McCloskey, B. D. Promising routes to a high Li^+ transference number electrolyte for lithium ion batteries. *ACS Energy Lett.* **2017**, *2*, 2563–2575.
[58] Li, M. N.; Zhang, Z. J.; Yin, Y. T.; Guo, W. C.; Bai, Y. G.; Zhang, F.; Zhao, B.; Shen, F.; Han, X. G. Novel polyimide separator prepared with two porogens for safe lithium-ion batteries. *ACS Appl. Mater. Interfaces* **2020**, *12*, 3610–3616.
[59] Liu, W.; Lin, D. C.; Pei, A.; Cui, Y. Stabilizing lithium metal anodes by uniform Li-ion flux distribution in nanochannel confinement. *J. Am. Chem. Soc.* **2016**, *138*, 15443–15450.
[60] Lu, Z. H.; Sui, F.; Miao, Y. E.; Liu, G. H.; Li, C.; Dong, W.; Cui, J.; Liu, T. X.; Wu, J. X.; Yang, C. L. Polyimide separators for rechargeable batteries. *J. Energy Chem.* **2021**, *58*, 170–197.

This is an open access article under the terms of the Creative Commons Attribution 4.0 International License (CC BY 4.0, https://creativecommons.org/licenses/by/4.0/).

© The Author(s) 2025. Published by Tsinghua University Press.